Rotating Multidimensional Quantum Droplets

Liangwei Dong[1,*] and Yaroslav V. Kartashov[2]
[1]Department of Physics, Shaanxi University of Science & Technology, Xi'an 710021, China
[2]Institute of Spectroscopy, Russian Academy of Sciences, Troitsk, Moscow, 108840, Russia

(Received 26 January 2021; revised 5 April 2021; accepted 10 May 2021; published 17 June 2021)

We predict a new type of two- and three-dimensional stable quantum droplets persistently rotating in broad external two-dimensional and weakly anharmonic potential. Their evolution is described by the system of the Gross-Pitaevskii equations with Lee-Huang-Yang quantum corrections. Such droplets resemble whispering-gallery modes localized in the polar direction due to nonlinear interactions and, depending on their chemical potential and rotation frequency, they appear in rich variety of shapes, ranging from nearly flat-top or strongly localized rotating wave packets, to crescentlike objects extending nearly over the entire range of polar angles. Above critical rotation frequency quantum droplets transform into vortex droplets (in two dimensions) or vortex tori (in three dimensions), whose topological charge gradually increase with the increase of the modulus of chemical potential, and therefore they belong to the family of nonlinear modes connecting fundamental and vortex quantum droplets. Rotating quantum droplets are exceptionally robust objects, stable practically in the entire range of their existence.

DOI: 10.1103/PhysRevLett.126.244101

Formation of multidimensional nonlinear localized waves is a problem of fundamental importance in diverse areas of physics. Various mechanisms supporting the formation of such states are known [1–4]. Quantum droplets, created in Bose-Einstein condensates (BECs), represent an intriguing example of self-sustained states, which can be stable in both two- and three-dimensional geometries. They are stabilized by the Lee-Huang-Yang (LHY) correction to the mean-field energy, induced by quantum fluctuations [5]. The possibility of suppression of collapse for Bose-Bose mixtures due to repulsive LHY correction was considered in Refs. [6,7], where stationary quantum droplets, filled by a nearly incompressible quantum liquid, were predicted. In binary mixtures [6,7] stabilization is possible when inter- and intraspecies interactions become nearly equal in magnitude, but opposite in sign, so that remaining small imbalance in favor of interspecies attraction may be counteracted by the competing LHY correction. Quantum droplets also exist in a single-component gas of dipolar atoms with long-range attractive interactions [8–16]. Creation of quantum droplets was reported in nearly 2D [17,18] and 3D [19,20] configurations using a mixture of two different atomic states in ^{39}K or attractive heteronuclear mixture of ^{41}K and ^{87}Rb atoms [21]. Such states exist also in the 1D geometry [7,22–24]. Droplets in two-component dipolar BECs are also under active investigation [25,26]. Dipolar condensates were used to demonstrate supersolidlike behavior of quantum droplets [27–32]. Spin-orbit coupling substantially enriches the physics of formation of quantum droplets [33–36].

LHY correction may also stabilize excited multidimensional states. Their properties depend on the dimensionality of the problem, since the form of the LHY correction changes upon reduction of the dimensionality. Among stable excited states, predicted so far, are 2D [37] and 3D [38] vortex quantum droplets. Their counterparts in dipolar condensates turn out to be unstable [39]. Vortices can be nested in arrays of quantum droplets in periodic potentials [40,41]. Stable droplets in binary mixtures may have different density profiles or vorticities in two components [37,42,43]. Quantum droplets in external potentials may aggregate into crystals [14] or vortex arrays [44] (akin to vortex lattices in repulsive condensates [45,46]), and form metastable clusters in free space [47]. The transition from the superfluid to the supersolid phases and to droplet crystals in rotating dipolar condensates in axially deformed traps was reported in Ref. [48]. Recent progress in this field is described in Ref. [49].

While the formation of various excited droplet configurations was predicted, there are no evidences that *single* quantum droplets can exist as stable objects performing persistent rotary motion in broad external potentials. The goal of this Letter is to introduce such rotating droplets in both 2D and 3D settings and to show that they can be stable. Rotating quantum droplets can be considered as whispering-gallery modes, confined in the polar direction by the nonlinear interactions. They represent a new family of localized nonlinear states, parametrized by the rotation frequency that connects nonrotating *fundamental* and *vortex* droplets. They resemble azimuthons [50–53], but differ from them, since azimuthons bifurcate from

antisymmetric dipole modes, while our single-spot states are strongly asymmetric.

We start our analysis from the 2D geometry, where the evolution of two components of binary BEC in broad external potential is described by coupled Gross-Pitaevskii equations [6,7] for dimensionless wave functions $\psi_{1,2}(x, y, t)$ (for details of normalization see Ref. [54]). We assume identical shapes of components $\psi_1 = \psi_2 = \psi$ and identical intraspecies interactions that allow us to reduce the full binary system to the equation

$$i\frac{\partial\psi}{\partial t} = -\frac{1}{2}\Delta_{2D}\psi + 2\sigma|\psi|^2\psi\ln(2|\psi|^2) + V\psi. \quad (1)$$

Here, $\Delta_{2D} = \partial^2/\partial x^2 + \partial^2/\partial y^2$, σ is the strength of the logarithmic LHY contribution to nonlinearity, while difference cubic nonlinearity vanishes for $\psi_1 = \psi_2 = \psi$. Potential $V = (-\alpha r^2 + \beta r^4)/2$, where r is the radial coordinate in the (x, y) plane, is anharmonic with $\alpha = 10^{-2}$, $\beta = 10^{-4}$. Its role consists in the creation of a shallow radial minimum that stimulates the formation of whispering-gallery modes, while LHY correction is responsible for stabilization of 2D states. Equation (1) conserves the total norm $N = 2\iint|\psi|^2 d^2\mathbf{r}$ and energy $\mathcal{E} = \iint\{|\nabla\psi|^2 + 2\sigma|\psi|^4\ln[2e^{-1/2}|\psi|^2] + 2V|\psi|^2\}d^2\mathbf{r}$. To find persistently rotating quantum droplets we use coordinate frame $x' = x\cos(\omega t) + y\sin(\omega t)$, $y' = y\cos(\omega t) - x\sin(\omega t)$ that rotates with frequency ω, where Eqs. (1) acquire the following form:

$$i\frac{\partial\psi}{\partial t} = -\frac{1}{2}\Delta_{2D}\psi + i\omega\left(x\frac{\partial\psi}{\partial y} - y\frac{\partial\psi}{\partial x}\right) + 2\sigma|\psi|^2\psi\ln(2|\psi|^2) + V\psi. \quad (2)$$

We omitted primes in coordinates in Eq. (2) and set $\sigma = 1$. The second term in the right-hand side of Eq. (2) accounts for the Coriolis force that can be counterbalanced by external potential V. Equating the potential force, $-dV/dr$, to the centripetal force $-\omega^2 r$, which supports circular motion with frequency ω, one obtains rough estimate for the droplet rotation radius, $r = [(\alpha + \omega^2)/2\beta]^{1/2}$.

Persistently rotating droplets can be found in the form $\psi = w(x, y)e^{-i\mu t}$, where w is the complex-valued function and μ is the chemical potential, when dispersion is arrested by the logarithmic nonlinearity (switching from self-attraction to repulsion with the increase of the density). The profiles of such droplets are shown in Fig. 1. Rotating quantum droplets are strongly asymmetric states, which always feature only one density maximum. Their phase is trivial at $\omega = 0$, but it acquires complex structure with multiple nested phase singularities, when rotation frequency increases. With an increase of the ω phase singularities come from transverse infinity and gradually approach the $r = 0$ point, around which the droplet rotates

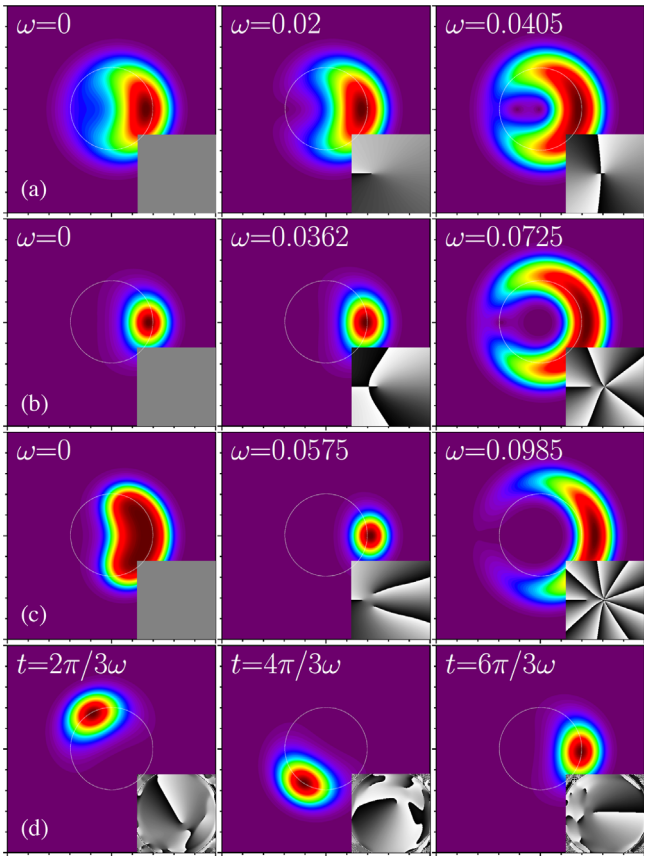

FIG. 1. Rotating quantum droplets for various ω at $\mu = -0.09$ (a), $\mu = -0.18$ (b), and $\mu = -0.35$ (c). Modulus of two identical components $|\psi_1| = |\psi_2| = |\psi|$ and phase distributions (insets) are shown within $x, y \in [-18, +18]$ windows. White circles indicate the potential minimum. (d) Stable rotation of quantum droplet with $\omega = 0.04$, $\mu = -0.18$.

[Figs. 1(a)–1(c)]. The number of singularities generally increases with increase of $|\mu|$. This process is accompanied by gradual expansion of the droplet in the polar direction, so that it acquires a pronounced crescentlike shape. At critical rotation frequency $\omega = \omega_m$ droplets become radially symmetric, while all phase singularities merge into a central one with topological charge m (see insets in Fig. 1). Therefore, the family of rotating droplets, parametrized by ω, connects families of asymmetric fundamental and radially symmetric vortex states. Rotating droplets appear in a variety of shapes ranging from crescentlike states [Fig. 1(a)], to well-localized spots [Fig. 1(b)], and flat-top modes [Fig. 1(c)]. In external potential V flat-top shapes emerge at $\mu_{cr} \approx \mu_u + \mu_0$, where $\mu_u = e^{-1/2}\ln e^{-1/2}$ is the critical value of the chemical potential in the uniform medium, at which droplets would acquire nearly constant density $\rho = e^{-1/2}$, and $\mu_0 \approx -0.0648$ is the eigenvalue of the fundamental linear mode of potential V with topological charge $m = 0$. Notice that with increase of ω such flat-top droplets first exhibit strong contraction and then acquire crescentlike shapes [Fig. 1(c)].

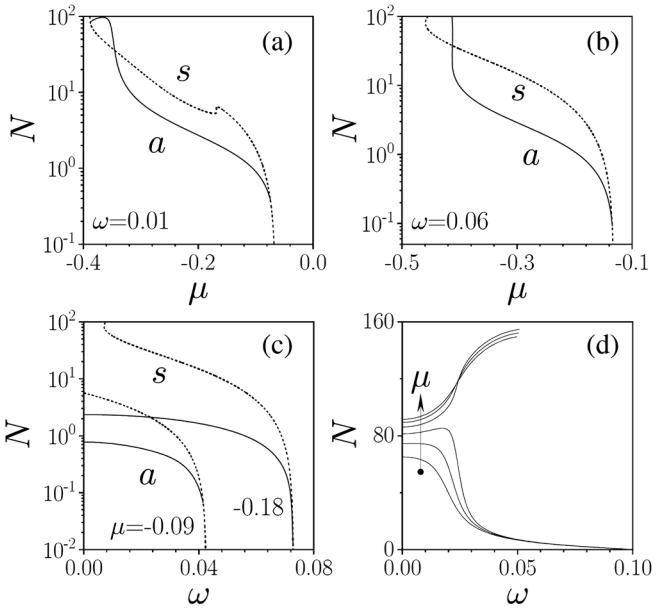

FIG. 2. (a) N versus μ for 2D rotating droplets and radially symmetric state with $m = 0$ at $\omega = 0.01$. Labels a and solid lines correspond to asymmetric rotating states, while labels s and dashed lines correspond to radially symmetric states. (b) N versus μ for rotating droplet and radially symmetric state with $m = 3$ at $\omega = 0.06$. (c) N versus rotation frequency ω at different μ values. Radial modes from which bifurcation occurs carry charges $m = 2$ ($\mu = -0.09$) and $m = 5$ ($\mu = -0.18$). (d) N versus ω for nearly flat-top 2D droplets (μ decreases along the arrow from -0.35 to -0.36 in steps of $\delta\mu = 0.002$).

The dependencies of norm N of 2D droplets on μ and ω are presented by solid lines in Figs. 2(a), 2(b) and Figs. 2(c), 2(d), respectively. For comparison, on the same plots we present also dependencies obtained for radially symmetric vortex modes $\psi = w(r)e^{im\phi - i\mu t}$ (here m is the topological charge) of Eq. (2) that coexist with rotating droplets (see dashed lines). One can see that with a decrease of $|\mu|$ or with increase of ω the family of asymmetric rotating droplets joins, at *nonzero* norm N, with radially symmetric family with certain topological charge m. The latter family, in turn, emerges under the action of nonlinearity from one of the linear eigenmodes of the potential V. The topological charge of radially symmetric family, from which rotating droplets bifurcate upon variation of ω [Fig. 2(c)], systematically increases with increase of $|\mu|$. This can be understood from Eq. (2), written in polar coordinates (r, ϕ):

$$i\frac{\partial\psi}{\partial t} - i\omega\frac{\partial\psi}{\partial\phi} = -\frac{1}{2}\left(\frac{\partial^2\psi}{\partial r^2} + \frac{1}{r}\frac{\partial\psi}{\partial r} + \frac{1}{r^2}\frac{\partial^2\psi}{\partial\phi^2}\right) + 2\sigma|\psi|^2\psi\ln(2|\psi|^2) + V\psi. \quad (3)$$

Substituting $\psi = w(r)e^{im\phi - i\mu t}$ into it shows that rotation has the only effect on radial solutions consisting in modification of chemical potential $\mu \to \mu + m\omega$, which for $m, \omega > 0$ is equivalent to a simple shift of corresponding $N(\mu)$ dependence by $m\omega$ in the negative direction of the μ axis. At the same time, radial families associated with increasing topological charges m bifurcate from linear modes of the anharmonic potential V at gradually increasing cutoff values $\mu_{m=0} \approx -0.0648$, $\mu_{m=1} \approx -0.0445$, $\mu_{m=2} \approx -0.0049$, $\mu_{m=3} \approx 0.0481$, etc. With an increase of rotation frequency ω, these families start to "override" each other in the negative μ direction due to the above-mentioned shift of the chemical potential $\sim m\omega$. Because cutoff values μ_m increase with m, the larger is the charge m; the larger frequency ω is needed for a given family to override the families with lower topological charges. We found that the family $N(\mu)$ of asymmetric *rotating* droplets joins (bifurcates) with that family of radially symmetric states, which was "met" first upon decrease of $|\mu|$ [see Figs. 2(a), 2(b)] and for larger rotation frequency ω this will be the family with larger topological charge m. This explains the phase structure of rotating droplets from Figs. 1(a)–1(c) around the $\omega = \omega_m$ value, where they transform into vortex states.

These observations are summarized in Fig. 3(a) in the form of the dependence of the maximal rotation frequency ω_m on chemical potential μ. Rotating 2D droplets exist for all frequencies below ω_m. At the upper edge of the existence domain in ω they transform into vortices whose topological charge grows by 1 between domains shown by the dots of different colors starting from $m = 0$ at $\mu \sim -0.0648$ up to $m = 9$ at $\mu \sim -0.355$ (i.e., when one moves from right to the left). With further increase of $|\mu|$ maximal frequency ω_m suddenly drops down and the existence domain shrinks. This is connected with qualitative modification of the $N(\omega)$ dependence for nearly flat-top states [Fig. 2(d)]. To analyze stability of 2D droplets we substituted perturbed profiles $\psi_{1,2} = (w_{1,2} + u_{1,2}e^{\delta t} + v_{1,2}^* e^{\delta^* t})e^{-i\mu t}$, where $u_{1,2}$, $v_{1,2} \ll w_{1,2}$, into Eq. (1),

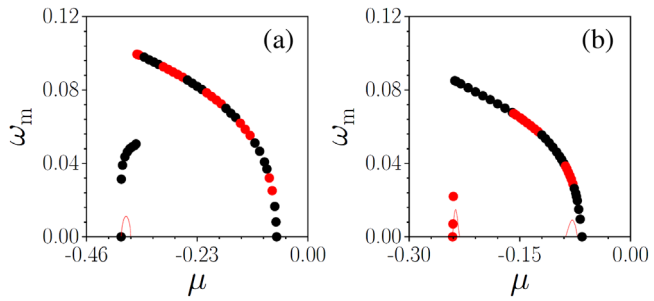

FIG. 3. Existence domains of the rotating 2D (a) and 3D (b) droplets on the (μ, ω) plane. Domains on the upper edge, where topological charge increases by 1 with an increase of $|\mu|$ are marked by the dots of a different color (for 2D states the charge at $\omega = \omega_m$ increases from $m = 0$ at $\mu \sim -0.0648$ up to $m = 9$ at $\mu \sim -0.355$, while for 3D states it increases up to $m = 4$ at $\mu \sim -0.238$). Droplets are unstable below red solid curves and are stable above them.

linearized it, and solved the resulting eigenvalue problem numerically to obtain the dependence of the perturbation growth rate δ on μ, ω. Only one narrow instability domain was detected, which is located below the red solid curve in Fig. 3(a). In the largest part of their existence domain rotating droplets are completely stable. The example of stable rotation is presented in Fig. 1(d) (only one rotation period is shown, but the dynamics remains periodic over huge times t).

Rotating asymmetric droplets can be encountered also in a 3D binary condensate, where their evolution for $\psi_1 = \psi_2 = \psi$ is governed by

$$i\frac{\partial\psi}{\partial t} = -\frac{1}{2}\Delta_{3D}\psi + [(1-g)|\psi|^2 + g_{\mathrm{LHY}}|\psi|^3]\psi + V\psi, \quad (4)$$

where the LHY correction $\sim g_{\mathrm{LHY}}$, whose form depends on dimensionality, now leads to additional quartic self-repulsion, g is the strength of the interspecies attraction, the strength of intraspecies repulsion is normalized to 1, $\Delta_{3D} = \partial^2/\partial x^2 + \partial^2/\partial y^2 + \partial^2/\partial z^2$, and the potential $V = (-\alpha r^2 + \beta r^4)/2$ is identical to the one used in the 2D case. To obtain rotating quantum droplets we move into the rotating with frequency ω [in the (x, y) plane] coordinate frame, and search there for stationary solutions of the form $\psi_{1,2} = \psi = w(x, y, z)e^{-i\mu t}$ using the Newton conjugate-gradients method. Because potential acts only in the (x, y) plane, such states are localized in the z direction only due to interparticle interactions. Typical dependencies of the norm $N = 2\iiint |\psi|^2 d^3\mathbf{r}$ of such states on chemical potential μ and rotation frequency ω are depicted in Figs. 4(a) and 4(b), respectively. As in the 2D case, families of asymmetric rotating droplets bifurcate from (join with) the families of radially symmetric states of the form $w(r, z)e^{im\phi - i\mu t}$. In the bifurcation point asymmetric 3D droplets may transform into *vortex tori*, i.e., localized states carrying vorticity in the (x, y) plane, with bell-shaped density distributions in the z direction (in which they considerably expand at low values of the norm). 3D rotating droplets become nearly radially symmetric also in the flat-top regime, at very large N values.

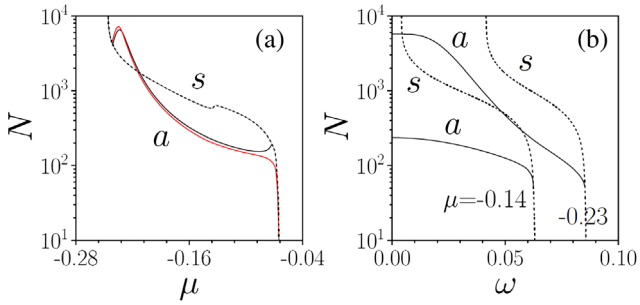

FIG. 4. (a) Norm N versus μ for 3D rotating droplets ($\omega = 0$—solid black curve, $\omega = 0.02$—solid red curve) and radially symmetric state with $m = 0$ (dashed curve). (b) N versus ω for rotating droplets (solid curves) and radially symmetric states (dashed curves) for various μ. Radially symmetric states, from which bifurcation occurs, carry topological charges $m = 3$ ($\mu = -0.14$) and $m = 4$ ($\mu = -0.23$). Here and below $g_{\mathrm{LHY}} = 0.5$, $g = 1.75$.

Representative shapes of the 3D asymmetric rotating droplets are presented in Fig. 5 in the form of isosurface plots. We show the state with nearly flat-top shape and large norm [Fig. 5(a)] and well-localized states with smaller norms [Figs. 5(b), 5(c)]. The tendency for transformation into crescentlike [in the (x, y) plane] modes and subsequently into vortex tori with increase of the rotation frequency ω is illustrated in Figs. 5(b), 5(c). Their phase distributions show the appearance of vortex lines moving to the origin in the (x, y) plane with increase of the rotation frequency. In Fig. 3(b) we show the domain of existence of 3D rotating droplets on the (μ, ω) plane. It is substantially narrower (in μ) than the analogous domain for 2D droplets [cf. Fig. 3(a)]. We were able to achieve the transformation of 3D rotating droplets (at $\omega = \omega_m$) into vortex tori with topological charges up to $m = 4$. This charge increases when one moves along the upper border of the existence domain in Fig. 3(b) from the right to the left, as in the 2D case.

Direct modeling of the evolution of 3D rotating droplets, slightly perturbed by input random noise, in the frames of

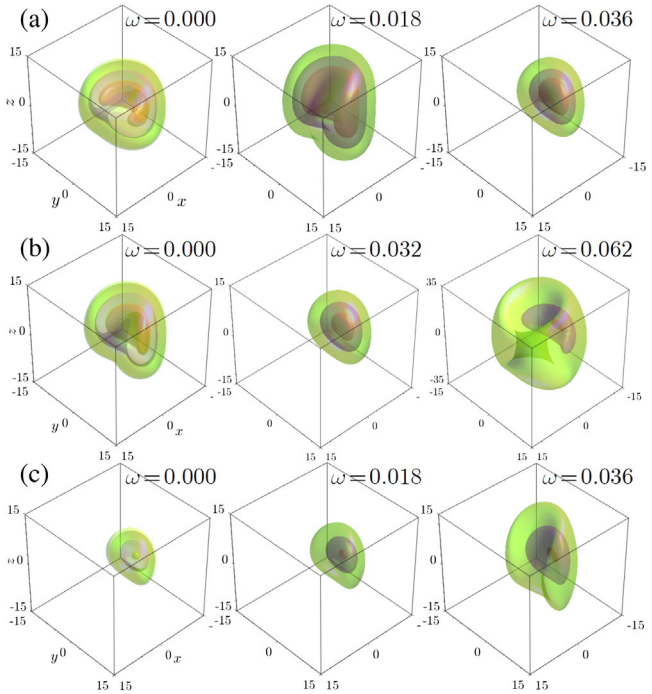

FIG. 5. Isosurface $|\psi|$ plots illustrating profiles of the 3D rotating droplets at (a) $\mu = -0.238$, (b) $\mu = -0.140$, and (c) $\mu = -0.088$ for different ω. Isosurface levels in (a),(c) are $0.10\psi_{\max}$, $0.55\psi_{\max}$, $0.95\psi_{\max}$, while in (b) they are $0.23\psi_{\max}$, $0.55\psi_{\max}$, $0.95\psi_{\max}$, where $\psi_{\max} = \max|\psi|$ for a given set of μ, ω parameters.

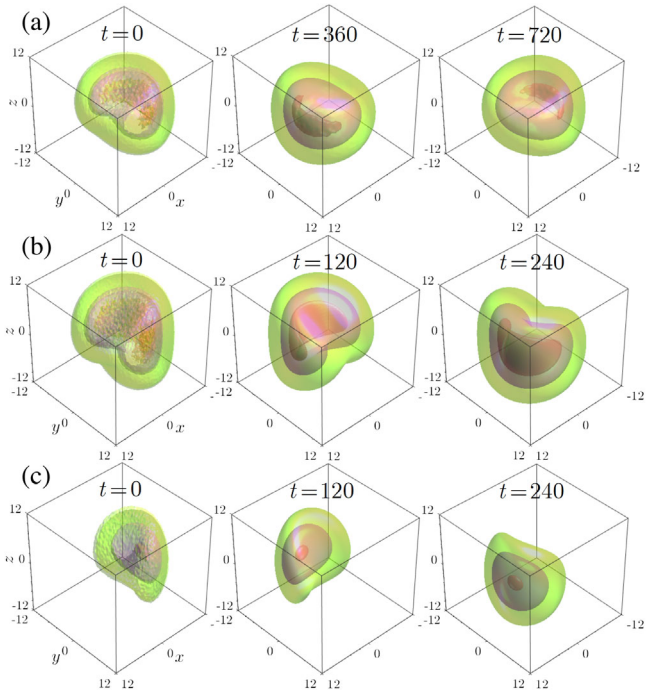

FIG. 6. Isosurface $|\psi|$ plots at different t illustrating unstable (a) and stable (b),(c) evolution of the perturbed 3D droplets. In (a) $\mu = -0.238$, $\omega = 0$; in (b) $\mu = -0.238$, $\omega = 0.014$; in (c) $\mu = -0.076$, $\omega = 0.014$. Isosurface levels in (a),(b) are $0.2\psi_{\max}$, $0.8\psi_{\max}$, $0.985\psi_{\max}$, while in (c) they are $0.2\psi_{\max}$, $0.55\psi_{\max}$, $0.95\psi_{\max}$.

Eq. (4) has shown that they are stable in the largest part of their existence domain. Only two narrow instability islands on the (μ, ω) plane were detected which are located below the red solid curve in Fig. 3(b). Importantly, this implies that rotating states close to vortex tori with topological charges 3 and 4 can be stable too (in free space only vortex tori with topological charges up to $m = 2$ were encountered [38]). Figure 6 illustrates examples of the unstable [Fig. 6(a)] and stable [Figs. 6(b), 6(c)] evolution of initially perturbed droplets (notice small-scale noise added into wave functions at $t = 0$). The unstable droplets exhibit long-living vibrations but do not collapse. In contrast, stable droplets show persistent rotation over very long times.

In a potential experiment the droplet may be initially prepared (using standard technique [17,19] based on tuning scattering lengths in the external magnetic field) in combination of two 2D traps: a weak anharmonic trap, where the droplet would rotate, and a displaced tighter trap initially holding the droplet around the minimum of the weak anharmonic trap (a similar approach has been used in Ref. [20]). Removal of the tighter trap and subsequent phase imprinting using an external vortical beam [55–57], will create droplet rotating in a weak anharmonic trap. Alternatively, a droplet can be kicked tangentially by an oblique beam. Rotating droplets do not require a flat-top regime for their stable evolution (they remain stable at sufficiently low norm values) and therefore they can be created in similar parameter range as states reported in Refs. [17,19]. We use normalized equations, where the scaled coordinates are $(x, y, z) = (Xr_0^{-1}, Yr_0^{-1}, Zr_0^{-1})$, r_0 is the characteristic spatial scale defining characteristic energy $\varepsilon_0 = \hbar^2/mr_0^2$ and time $t_0 = \hbar\varepsilon_0^{-1}$ scales ($t = Tt_0^{-1}$), m is the atomic mass, nonlinear coefficients $g = |g_x|g_s^{-1}$ and $g_{\mathrm{LHY}} = 4\varepsilon_0^{1/2}(2m)^{3/2}/3\pi^2\hbar^3$, where $g_s = 4\pi\hbar^2 a_{11}/m = 4\pi\hbar^2 a_{22}/m > 0$ and $g_x = 4\pi\hbar^2 a_{12}/m < 0$ are the coupling constants characterizing intracomponent repulsion and intercomponent attraction, a_{11}, a_{22}, a_{12} are scattering lengths, the wave function is scaled as $(g_s/\varepsilon_0)^{1/2}\Psi = \psi$, the parameters of the external potential V are $\alpha = m\omega^2 r_0^2/\varepsilon_0$ and $\beta = \lambda m\omega^2 r_0^4/\varepsilon_0 d^2$, where ω is the trapping frequency, $d = (\hbar/m\omega)^{1/2}$ is the oscillator length, and λ is the small anharmonicity parameter (for details see Ref. [54]). Dimensionless norm N is related to a number of atoms $\mathcal{N}$ in the condensate as $\mathcal{N} = (\varepsilon_0 r_0^3/g_s)N$.

Summarizing, we introduced a new type of the rotating quantum droplets in both 2D and 3D systems that connect the families of fundamental and vortex droplets. They demonstrate remarkable stability and appear in a variety of shapes. Such multidimensional states can be potentially encountered in other areas, including nonlinear optics, not only in conservative, but also in dissipative systems.

*dongliangwei@sust.edu.cn

[1] B. A. Malomed, D. Mihalache, F. Wise, and L. Torner, Spatiotemporal optical solitons, J. Opt. B **7**, R53 (2005).
[2] R. Carretero-Gonzalez, D. J. Frantzeskakis, and P. G. Kevrekidis, Nonlinear waves in Bose-Einstein condensates: Physical relevance and mathematical techniques, Nonlinearity **21**, R139 (2008).
[3] V. S. Bagnato, D. J. Frantzeskakis, P. G. Kevrekidis, B. A. Malomed, and D. Mihalache, Bose-Einstein condensation: Twenty years after, Romanian Reports in Physics **67**, 5 (2015), http://www.rrp.infim.ro/2015_67_1.html.
[4] Y. V. Kartashov, G. Astrakharchik, B. Malomed, and L. Torner, Frontiers in multidimensional self-trapping of nonlinear fields and matter, Nat. Rev. Phys. **1**, 185 (2019).
[5] T. D. Lee, K. Huang, and C. N. Yang, Eigenvalues and eigenfunctions of a Bose system of hard spheres and its low-temperature properties, Phys. Rev. **106**, 1135 (1957).
[6] D. S. Petrov, Quantum Mechanical Stabilization of a Collapsing Bose-Bose Mixture, Phys. Rev. Lett. **115**, 155302 (2015).
[7] D. S. Petrov and G. E. Astrakharchik, Ultradilute Low-Dimensional Liquids, Phys. Rev. Lett. **117**, 100401 (2016).
[8] M. Schmitt, M. Wenzel, F. Böttcher, I. Ferrier-Barbut, and T. Pfau, Self-bound droplets of a dilute magnetic quantum liquid, Nature (London) **539**, 259 (2016).
[9] I. Ferrier-Barbut, H. Kadau, M. Schmitt, M. Wenzel, and T. Pfau, Observation of Quantum Droplets in a Strongly Dipolar Bose Gas, Phys. Rev. Lett. **116**, 215301 (2016).

[10] F. Böttcher, M. Wenzel, J.-N. Schmidt, M. Guo, T. Langen, I. Ferrier-Barbut, T. Pfau, R. Bombín, J. Sánchez-Baena, J. Boronat, and F. Mazzanti, Dilute dipolar quantum droplets beyond the extended Gross-Pitaevskii equation, Phys. Rev. Research **1**, 033088 (2019).

[11] F. Wächtler and L. Santos, Ground-state properties and elementary excitations of quantum droplets in dipolar Bose-Einstein condensates, Phys. Rev. A **94**, 043618 (2016).

[12] D. Baillie, R. M. Wilson, R. N. Bisset, and P. B. Blakie, Self-bound dipolar droplet: A localized matter wave in free space, Phys. Rev. A **94**, 021602(R) (2016).

[13] L. Chomaz, S. Baier, D. Petter, M. J. Mark, F. Wächtler, L. Santos, and F. Ferlaino, Quantum-Fluctuation-Driven Crossover from a Dilute Bose-Einstein Condensate to a Macrodroplet in a Dipolar Quantum Fluid, Phys. Rev. X **6**, 041039 (2016).

[14] D. Baillie and P. B. Blakie, Droplet Crystal Ground States of a Dipolar Bose Gas, Phys. Rev. Lett. **121**, 195301 (2018).

[15] A. Cidrim, F. E. A. dos Santos, E. A. L. Henn, and T. Macrí, Vortices in self-bound dipolar droplets, Phys. Rev. A **98**, 023618 (2018).

[16] D. Baillie and P. B. Blakie, Droplet Crystal Ground States of a Dipolar Bose Gas, Phys. Rev. Lett. **121**, 195301 (2018).

[17] C. R. Cabrera, L. Tanzi, J. Sanz, B. Naylor, P. Thomas, P. Cheiney, and L. Tarruell, Quantum liquid droplets in a mixture of Bose-Einstein condensates, Science **359**, 301 (2018).

[18] P. Cheiney, C. R. Cabrera, J. Sanz, B. Naylor, L. Tanzi, and L. Tarruell, Bright Soliton to Quantum Droplet Transition in a Mixture of Bose-Einstein Condensates, Phys. Rev. Lett. **120**, 135301 (2018).

[19] G. Semeghini, G. Ferioli, L. Masi, C. Mazzinghi, L. Wolswijk, F. Minardi, M. Modugno, G. Modugno, M. Inguscio, and M. Fattori, Self-Bound Quantum Droplets of Atomic Mixtures in Free Space, Phys. Rev. Lett. **120**, 235301 (2018).

[20] G. Ferioli, G. Semeghini, L. Masi, G. Giusti, G. Modugno, M. Inguscio, A. Gallemí, A. Recati, and M. Fattori, Collisions of Self-Bound Quantum Droplets, Phys. Rev. Lett. **122**, 090401 (2019).

[21] C. D'Errico, A. Burchianti, M. Prevedelli, L. Salasnich, F. Ancilotto, M. Modugno, F. Minardi, and C. Fort, Observation of quantum droplets in a heteronuclear bosonic mixture, Phys. Rev. Research **1**, 033155 (2019).

[22] G. E. Astrakharchik and B. A. Malomed, Dynamics of one-dimensional quantum droplets, Phys. Rev. A **98**, 013631 (2018).

[23] F. K. Abdullaev, A. Gammal, R. K. Kumar, and L. Tomio, Faraday waves and droplets in quasi-one-dimensional Bose gas mixtures, J. Phys. B **52**, 195301 (2019).

[24] S. R. Otajonov, E. N. Tsoy, and F. K. Abdullaev, Stationary and dynamical properties of one-dimensional quantum droplets, Phys. Lett. A **383**, 125980 (2019).

[25] R. N. Bisset, L. A. Peña Ardila, and L. Santos, Quantum Droplets of Dipolar Mixtures, Phys. Rev. Lett. **126**, 025301 (2021).

[26] J. C. Smith, D. Baillie, and P. B. Blakie, Quantum Droplet States of a Binary Magnetic Gas, Phys. Rev. Lett. **126**, 025302 (2021).

[27] L. Tanzi, S. M. Roccuzzo, E. Lucioni, F. Famà, A. Fioretti, C. Gabbanini, G. Modugno, A. Recati, and S. Stringari, Supersolid symmetry breaking from compressional oscillations in a dipolar quantum gas, Nature (London) **574**, 382 (2019).

[28] M. Guo, F. Boettcher, J. Hertkorn, J. N. Schmidt, M. Wenzel, H. P. Büchler, T. Langen, and T. Pfau, The low-energy Goldstone mode in a trapped dipolar supersolid, Nature (London) **574**, 386 (2019).

[29] F. Boettcher, J.-N. Schmidt, M. Wenzel, J. Herkorn, M. Y. Guo, T. Langen, and T. Pfau, Transient Supersolid Properties in an Array of Dipolar Quantum Droplets, Phys. Rev. X **9**, 011051 (2019).

[30] L. Chomaz, D. Petter, P. Ilzhöfer, G. Natale, A. Trautmann, C. Politi, G. Durastante, R. M. W. van Bijnen, A. Patscheider, M. Sohmen, M. J. Mark, and F. Ferlaino, Long-Lived and Transient Supersolid Behaviors in Dipolar Quantum Gases, Phys. Rev. X **9**, 021012 (2019).

[31] L. Tanzi, E. Lucioni, F. Fama, J. Catani, A. Fioretti, C. Gabbaninin, R. N. Bisset, L. Santos, and G. Modugno, Observation of a Dipolar Quantum Gas with Metastable Supersolid Properties, Phys. Rev. Lett. **122**, 130405 (2019).

[32] G. Natale, R. M. W. van Bijnen, A. Patscheider, D. Petter, M. J. Mark, L. Chomaz, and F. Ferlaino, Excitation Spectrum of a Trapped Dipolar Supersolid and its Experimental Evidence, Phys. Rev. Lett. **123**, 050402 (2019).

[33] Y. Li, Z. Luo, Y. Liu, Z. Chen, C. Huang, S. Fu, H. Tan, and B. A. Malomed, Two-dimensional solitons and quantum droplets supported by competing self- and cross-interactions in spin-orbit-coupled condensates, New J. Phys. **19**, 113043 (2017).

[34] A. Tononi, Y. M. Wang, and L. Salasnich, Quantum solitons in spin-orbit-coupled Bose-Bose mixtures, Phys. Rev. A **99**, 063618 (2019).

[35] X. L. Cui, Spin-orbit-coupling-induced quantum droplet in ultracold Bose-Fermi mixtures, Phys. Rev. A **98**, 023630 (2018).

[36] J. Sanchez-Baena, J. Boronat, and F. Mazzanti, Supersolid striped droplets of a Raman spin-orbit-coupled system, Phys. Rev. A **102**, 053308 (2020).

[37] Y. Li, Z. Chen, Z. Luo, C. Huang, H. Tan, W. Pang, and B. A. Malomed, Two-dimensional vortex quantum droplets, Phys. Rev. A **98**, 063602 (2018).

[38] Y. V. Kartashov, B. A. Malomed, L. Tarruell, and L. Torner, Three-dimensional droplets of swirling superfluids, Phys. Rev. A **98**, 013612 (2018).

[39] A. Cidrim, F. E. A. dos Santos, E. A. L. Henn, and T. Macrí, Vortices in self-bound dipolar droplets, Phys. Rev. A **98**, 023618 (2018).

[40] X. L. Zhang, X. X. Xu, Y. Y. Zheng, Z. P. Chen, B. Liu, C. Q. Huang, B. A. Malomed, and Y. Y. Li, Semidiscrete Quantum Droplets and Vortices, Phys. Rev. Lett. **123**, 133901 (2019).

[41] Y. Y. Zheng, S. T. Chen, Z. P. Huang, S. X. Dai, B. Liu, Y. Y. Li, and S. R. Wang, Quantum droplets in two-dimensional optical lattices, Front. Phys. **16**, 22501 (2020).

[42] T. Mithun, A. Maluckov, K. Kasamatsu, B. Malomed, and A. Khare, Inter-component asymmetry and formation of quantum droplets in quasi-one-dimensional binary Bose gases, Symmetry **12**, 174 (2020).

[43] Y. V. Kartashov, B. A. Malomed, and L. Torner, Structured heterosymmetric quantum droplets, Phys. Rev. Research **2**, 033522 (2020).

[44] M. N. Tengstrand, P. Stürmer, E. Ö. Karabulut, and S. M. Reimann, Rotating Binary Bose-Einstein Condensates and Vortex Clusters in Quantum Droplets, Phys. Rev. Lett. **123**, 160405 (2019).

[45] A. L. Fetter, Rotating trapped Bose-Einstein condensates, Rev. Mod. Phys. **81**, 647 (2009).

[46] H. Saarikoski, S. M. Reimann, A. Harju, and M. Manninen, Vortices in quantum droplets: Analogies between boson and fermion systems, Rev. Mod. Phys. **82**, 2785 (2010).

[47] Y. V. Kartashov, B. A. Malomed, and L. Torner, Metastability of Quantum Droplet Clusters, Phys. Rev. Lett. **122**, 193902 (2019).

[48] S. M. Roccuzzo, A. Gallemí, A. Recati, and S. Stringari, Rotating a Supersolid Dipolar Gas, Phys. Rev. Lett. **124**, 045702 (2020).

[49] Z. H. Luo, W. Pang, B. Liu, Y. Y. Li, and B. A. Malomed, A new form of liquid matter: Quantum droplets, Front. Phys. **16**, 32201 (2021).

[50] A. S. Desyatnikov, A. A. Sukhorukov, and Y. S. Kivshar, Azimuthons: Spatially Modulated Vortex Solitons, Phys. Rev. Lett. **95**, 203904 (2005).

[51] V. M. Lashkin, Two-dimensional multisolitons and azimuthons in Bose-Einstein condensates, Phys. Rev. A **77**, 025602 (2008).

[52] V. M. Lashkin, Stable three-dimensional spatially modulated vortex solitons in Bose-Einstein condensates, Phys. Rev. A **78**, 033603 (2008).

[53] V. M. Lashkin, A. S. Desyatnikov, E. A. Ostrovskaya, and Y. S. Kivshar, Azimuthal vortex clusters in Bose-Einstein condensates, Phys. Rev. A **85**, 013620 (2012).

[54] See Supplemental Material at http://link.aps.org/supplemental/10.1103/PhysRevLett.126.244101 for description of dimensionless units and details of normalization of governing Gross-Pitaevskii equations.

[55] Ł. Dobrek, M. Gajda, M. Lewenstein, K. Sengstock, G. Birkl, and W. Ertmer, Optical generation of vortices in trapped Bose-Einstein condensates, Phys. Rev. A **60**, R3381 (1999).

[56] J. Denschlag, J. E. Simsarian, D. L. Feder, C. W. Clark, L. A. Collins, J. Cubizolles, L. Deng, E. W. Hagley, K. Helmerson, W. P. Reinhardt, S. L. Rolston, B. I. Schneider, and W. D. Phillips, Generating solitons by phase engineering of a Bose-Einstein condensate, Science **287**, 97 (2000).

[57] A. E. Leanhardt, A. Gorlitz, A. P. Chikkatur, D. Kielpinski, Y. Shin, D. E. Pritchard, and W. Ketterle, Imprinting Vortices in a Bose-Einstein Condensate Using Topological Phases, Phys. Rev. Lett. **89**, 190403 (2002).